

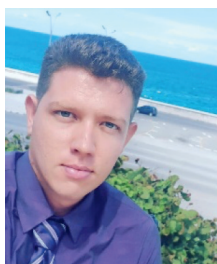
Probing Complex Photophysics in Gold Nanoclusters

Luis E. Llanes-Montesino^{*,a}, Gonzalo Angulo^b, Jiangtao Zhao^a, Thomas Bürgi^a, and Arnulf Rosspeintner^{*,a}

[§]SCS-dsm-firmenich Award for the Best Poster Presentation in Physical Chemistry

Abstract: We report striking photophysical behaviour of Au₂₅(PET)₁₈ (PET = 2-phenylethanethiol) nanoclusters in both anionic and neutral forms. Using broad spectral coverage and tuneable excitation, steady-state, and time-resolved measurements reveal low-energy absorption and emission features, weak photoluminescence, and multiexponential decay dynamics. Notably, the neutral species shows excitation-wavelength-dependent emissions and a pronounced mismatch between excitation and absorption spectra, violating Kasha's and Vavilov's rules. These results point towards complex excited-state behaviour of these systems and the crucial role of instrumentation design in their accurate characterisation.

Keywords: Excitation dynamics · Gold nanocluster · Luminescence · Photophysics



Luis Enrique Llanes Montesino is a PhD student in the Department of Physical Chemistry at the University of Geneva. He joined the research group of Prof. Thomas Bürgi in 2022 to pursue his doctoral studies. His work focuses on the photophysics and photochemistry of metal nanoclusters, using steady-state and time-resolved spectroscopy.

1. Introduction

Atomically precise metal nanoclusters (NCs), particularly gold nanoclusters (AuNCs), have gained significant attention due to their unique and versatile properties. Their relatively straightforward synthesis, coupled with precise size control and surface modification capabilities, has established them as a promising new class of materials.^[1–3] Of particular interest, from a fundamental perspective, is their monodispersity, a characteristic that sets them apart from other nano-sized species. This monodispersity enables the study of their intrinsic properties without the complications of size or composition distribution, facilitating clear experimental observations, similar to the study of molecules.^[4–6]

While mass spectrometry, diffraction techniques, and vibrational spectroscopies^[7] have been essential for determining the atomic and structural features of AuNCs, progress in understanding their electronic structure and optical properties, particularly their photophysics and excited-state dynamics, has been comparatively slow and often based on limited experimental data.^[8–10] This limits their practical use in photocatalytic, solar energy conversion, biological sensing, and imaging applications.^[11–14]

Our main concern with the existing literature in this area is the scarcity of systematic and comprehensive studies. In many cases, absorption and emission spectra do not cover a sufficiently large wavelength range, mainly due to the limited near-infrared (NIR) sensitivity of the silicon-based detectors of most commercial fluorimeters and absorption spectrometers. This is particularly critical given that available reports^[15] already indicate that many gold

nanoclusters exhibit electronic absorption and emission bands extending into the short-wave infrared. Similarly, excited-state dynamics are often oversimplified because of a limited dynamic range and a restricted temporal window of standard setups based on time-correlated single photon counting in the spectral region of interest (700–1400 nm), even though time-resolved emission data suggests dynamics spanning several orders of magnitude, from hundreds of picoseconds to tens of microseconds.^[15–18]

Here, we present the reasons why extended measurements are needed and how to perform them using dedicated devices to overcome the abovementioned limitations, enabling reliable measurement of AuNCs' photophysical properties and accurate characterisation of their emission features and excited-state dynamics.

2. Au₂₅(PET)₁₈ Nanoclusters

Au₂₅(2-phenylethanethiol)₁₈ nanoclusters (Fig. 1), in both anionic (Au₂₅[–]) and neutral (Au₂₅⁰) forms, were selected to showcase the necessity of the experimental approach for three key reasons: (i) their photophysics is the most extensively studied among AuNCs, (ii) their atomic structure is well-defined, and (iii) the thiolate ligands provide stability through strong Au–S bonds comparable to Au–Au interactions. These clusters were synthesised and purified according to previous reports,^[19] and their preparation and high purity confirmed by high-resolution electrospray ionisation mass spectrometry and matrix-assisted laser desorption/ionisation time-of-flight mass spectrometry. Purification, critical for reliable photophysical measurements, was achieved by passing the samples multiple times through a size-exclusion column.

3. Absorption Spectroscopy

Previous studies on Au₂₅(PET)₁₈ nanoclusters have reported charge-state-dependent absorption properties. For the negatively charged species, the lowest-energy absorption band is consistently observed at approximately 800 nm and is commonly assigned to the HOMO–LUMO transition.^[15,21,22] In contrast, the neutral cluster has shown more controversial behaviour, with most reports placing its lowest-energy absorption feature at

*Correspondence: L. Llanes-Montesino, E-mail: luis.llanesmontesino@unige.ch; Dr. A. Rosspeintner, E-mail: arnulf.rosspeintner@unige.ch

^aDepartment of Physical Chemistry, Faculty of Sciences (II), University of Geneva, 30 quai Ernest-Ansermet, CH-1211 Genève 4, Switzerland; ^bInstitute of Physical Chemistry, Polish Academy of Sciences, Kasprzaka 44/52, 01-224 Warsaw, Poland.

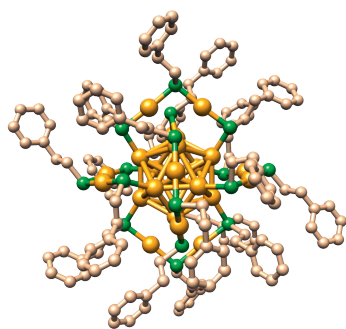


Fig. 1. X-ray diffraction derived structure of $[\text{Au}_{25}(\text{2-phenylethanethiol})_{18}]^0$. Au: gold, S: green, C: beige.^[20]

around 700 nm,^[22–25] based on measurements performed over a limited spectral range (<1000 nm).

Accurate characterisation of these low-energy absorption features requires optical measurements extending well into the NIR region and covering a large dynamic range. To meet these requirements, absorption spectra were recorded using a double-beam UV–Vis–NIR spectrophotometer (Varian Cary 5000), the additional PbS detector of which enables measurements over a broad spectral range up to 3300 nm, with a large dynamic range.

Within this extended range, the absorption spectrum of Au_{25}^- , shows a low-energy band at approximately 800 nm (Fig. 2, lower panel), in agreement with previous reports. In contrast, the neutral cluster exhibits two low-energy absorption features at approximately 950 and 1130 nm (Fig. 2, upper panel), which differs from earlier reports.

4. Luminescence Spectroscopy

The low emission quantum yields for both NCs (approximately 0.075% for the neutral form^[25] and about 1% for the negatively charged species^[18]) make the acquisition of high-quality emission data in the low-energy region using conventional light sources particularly challenging. In standard excitation configurations of commercial spectrofluorimeters (Horiba Nanolog), the excitation intensity drops sharply beyond 600 nm due to the wavelength-dependent efficiency of the excitation grating. This limitation is

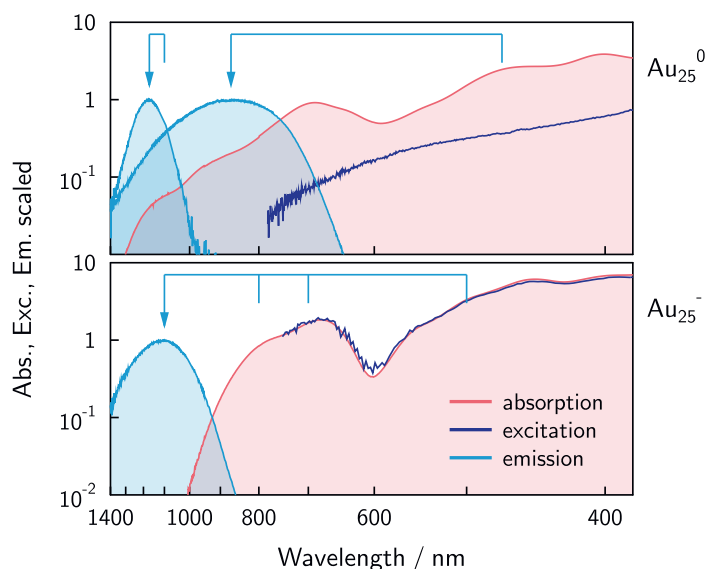


Fig. 2. Absorption, excitation, and emission spectra of Au_{25}^0 in dichloromethane (upper panel) and Au_{25}^- in acetonitrile (lower panel). The origin(s) of the blue arrow(s) indicate(s) the excitation wavelength(s) used to collect the emission spectra.

further exacerbated by (i) constraints on sample concentration, arising from the relatively high cost, (ii) moderate yields of synthesis and purification, as well as (iii) the limited solubility of the NC in organic solvents. Moreover, prolonged excitation times are undesirable due to the risk of photodecomposition.

To address these challenges, we used a home-built emission set-up employing pulsed white-light lasers (NKT, SuperK Extreme / SuperK Compact) coupled to a tuneable acousto-optic transmissive filter as the excitation source. The emission was collected in a 180° back-scattering geometry using a Cassegrain objective relayed *via* fibre bundles to a double-prism spectrograph (courtesy of Niko Ernsting)^[27] and a CCD camera (Princeton Instruments, PIXIS 2K) for the visible range and a grating spectrograph and an InGaAs photodiode array (ANDOR, iDus 1.7) for the near-infrared (Fig. 3). The very same optical geometry, including excitation, was also used for time-resolved measurements, differing only in the fibre-coupled detection devices (see Sec. 5).

This configuration provides (i) high-intensity, broadband tuneable excitation (470 – 1100 nm), (ii) front-face illumination minimising secondary inner filter effects,^[28] (iii) an achromatic detection path with a collection efficiency ($\text{NA} > 0.2$) comparable to the best state-of-the-art commercial apparatuses, and (iv) fibre-coupled broadband detectors enabling versatile, fast measurements.

4.1 Au_{25}^-

The emission spectrum consists of a single band centred at approximately 1100 nm (Fig. 2, lower panel), similar to previously reported data.^[15] Earlier observations of additional blue-shifted features^[29] are likely due to impurities, as confirmed by measurements on different chromatographic fractions showing identical absorption spectra.^[15,21]

4.2 Au_{25}^0

Excitation at 470 nm results in a broad emission band with a maximum centred at approx. 870 nm, in agreement with previous

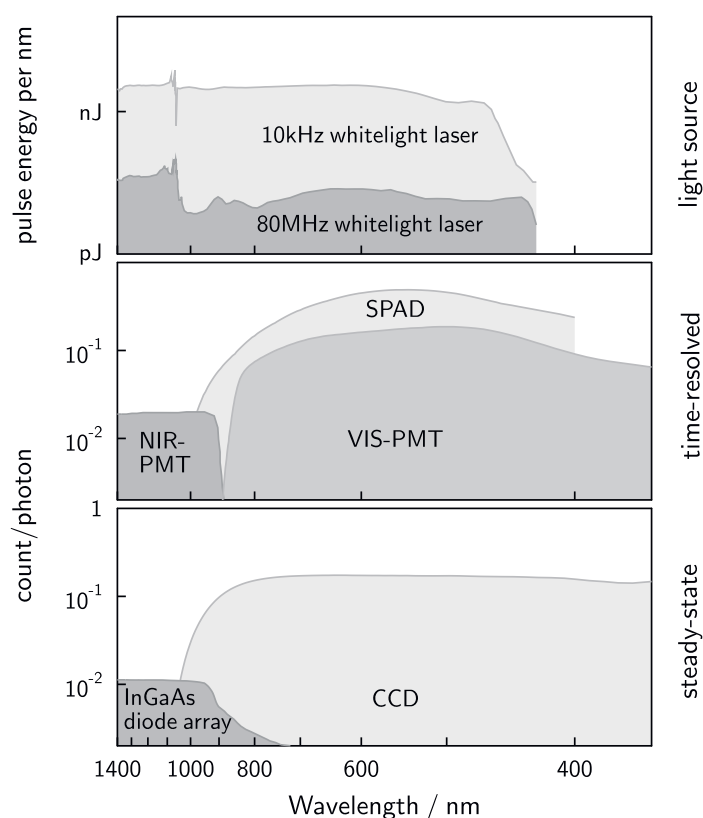


Fig. 3. Ranges covered by the light sources and detectors used for the time-resolved and steady-state measurements.

reports.^[16] This emission significantly overlaps with the low-energy absorption features. The sample was therefore also excited within this previously unreported absorption region. This results in a completely different narrow emission band centred around 1170 nm (Fig. 2, upper panel). This strong excitation wavelength dependence of the emission represents a clear violation of Kasha's rule.

4.3 Excitation Spectra

Excitation spectra were collected using a commercial spectrofluorimeter equipped with a liquid-nitrogen-cooled photomultiplier tube (Hamamatsu R5509-73), covering the range from 350 to 800 nm. Au_{25}^0 exhibits a clear mismatch between absorption and excitation spectra across the entire spectral range examined (Fig. 2, upper panel). This finding is not unexpected, given the excitation wavelength dependent emission spectra and indicates that not all excited states contribute equally to the observed emission, implying a violation of Vavilov's rule. In contrast, Au_{25}^- shows fully congruent absorption and excitation profiles (Fig. 2, lower panel), consistent with previous reports.^[15,16] These findings demonstrate that the negatively charged species follows conventional photophysics, whereas this is not the case for the neutral form.

5. Photoluminescence Decays

Time-resolved data were recorded with the same home-built setup we described above using time-correlated single-photon counting (Picoquant, PicoHarp 300) and multichannel scaling (Picoquant, Multiharp 150 N). For the detection, two photomultiplier tubes (PMT) covering the visible (Picoquant, PMA 192-C) and near-infrared (Hamamatsu H10330B-75) regions were used, together with a single-photon avalanche diode (SPAD, MPD, MPD-100-CTB) detector with remarkably low 15 dark counts per second. This detector/detection electronics combination allows for an exceptional dynamic range of 4 to 5 orders of magnitude while guaranteeing an extended temporal range of 5 to 6 orders of magnitude (see Fig. 4). This feature is particularly advantageous for the investigation of AuNCs exhibiting intrinsically weak and long-lived luminescence signals.

As shown in Fig. 4, the decay curve of Au_{25}^- can be well described by a monoexponential function, yielding a PL lifetime of 160 ns, in good agreement with previously reported values.^[15,25]

Au_{25}^0 exhibits strongly multi- or non-exponential behaviour (Fig. 4), with lifetimes ranging from sub-nanoseconds to several microseconds. This motivates time-resolved emission spectra (TRES) measurements across the emission band, for which the broad spectral coverage of the multiple detectors is necessary (Fig. 3). Given the excitation-dependent behaviour and long emission decays, performing TRES at different excitation energies is

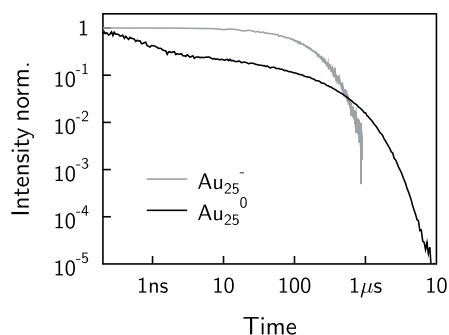


Fig. 4. Photoluminescence decays of Au_{25}^0 in dichloromethane (excitation: 500 nm, emission: 890 nm, SPAD) and Au_{25}^- in acetonitrile (excitation: 800 nm, emission: 1100 nm, NIR-PMT). The different dynamic ranges are a consequence of the different detectors.

also essential, highlighting the need for a tuneable low-repetition rate (<10 kHz) pulsed excitation source (SuperK Compact).

Notably, the decay traces presented here span a wide range in dynamic intensity as well as an extended temporal window, both of which are required to capture the full emission dynamics of these AuNCs.

6. Conclusions

In this work we argue that an extended spectral coverage and high-sensitivity detection are quintessential requirements for obtaining a reliable experimental basis to understand the photo-physics of gold nanoclusters. Access to the near-infrared reveals low-energy absorption and emission features, particularly in the neutral species, that are inaccessible with conventional setups. The combination of tuneable high-power excitation, achromatic collection optics, and low-noise detection enables the resolution of weak signals and complex excited-state dynamics with high dynamic range. These capabilities highlight the critical role of careful experimental design in elucidating the optical behaviour of Au_{25} NCs.

Acknowledgements

We are grateful to the Swiss Chemical Society and to dsm-firmenich for the best poster presentation award. This work was supported by the National Science Centre of Poland (grant OPUS-LAP 2021/43/I/ST4/01411), the University of Geneva and the Swiss National Science Foundation (grant 209554).

Received: February 14, 2026

- [1] M. Zhou, R. Jin, *Annu. Rev. Phys. Chem.* **2021**, *72*, 121, <https://doi.org/10.1146/annurev-physchem-090419-104921>.
- [2] I. Chakraborty, T. Pradeep, *Chem. Rev.* **2017**, *117*, 8208, <https://doi.org/10.1021/acs.chemrev.6b00769>.
- [3] T. Tsukuda, *Bull. Chem. Soc. Jpn.* **2012**, *85*, 151, <https://doi.org/10.1246/bcsj.20110227>.
- [4] R. Jin, H. Qian, Z. Wu, Y. Zhu, M. Zhu, A. Mohanty, N. Garg, *J. Phys. Chem. Lett.* **2010**, *1*, 2903, <https://doi.org/10.1021/jz100944k>.
- [5] D. A. Pichugina, N. E. Kuz'menko, A. F. Shestakov, *Russ. Chem. Rev.* **2015**, *84*, 1114, <https://doi.org/10.1070/RCR4493>.
- [6] M. Farrag, M. Tschurl, M. Dass, U. Heiz, *Phys. Chem. Chem. Phys.* **2013**, *15*, 12539, <https://doi.org/10.1039/c3cp51406d>.
- [7] B. Nieto-Ortega, T. Bürgi, *Acc. Chem. Res.* **2018**, *51*, 2811, <https://doi.org/10.1021/acs.accounts.8b00376>.
- [8] R. Jin, *Nanoscale* **2015**, *7*, 1549, <https://doi.org/10.1039/C4NR05794E>.
- [9] P. Yu, X. Wen, Y.-R. Toh, X. Ma, J. Tang, *Part. Part. Syst. Charact.* **2015**, *32*, 142, <https://doi.org/10.1002/ppsc.201400040>.
- [10] X. Kang, M. Zhu, *Chem. Soc. Rev.* **2019**, *48*, 2422, <https://doi.org/10.1039/C8CS00800K>.
- [11] V. N. Mehta, M. L. Desai, H. Basu, R. Kumar Singhal, S. K. Kailasa, *J. Mol. Liq.* **2021**, *333*, 115950, <https://doi.org/10.1016/j.molliq.2021.115950>.
- [12] Y. Zhang, C. Zhang, C. Xu, X. Wang, C. Liu, G. I. N. Waterhouse, Y. Wang, H. Yin, *Talanta* **2019**, *200*, 432, <https://doi.org/10.1016/j.talanta.2019.03.068>.
- [13] M. A. Abbas, P. V. Kamat, J. H. Bang, *ACS Energy Lett.* **2018**, *3*, 840, <https://doi.org/10.1021/acsenerylett.8b00070>.
- [14] Y. Du, H. Sheng, D. Astruc, M. Zhu, *Chem. Rev.* **2020**, *120*, 526, <https://doi.org/10.1021/acs.chemrev.8b00726>.
- [15] Z. Liu, M. Zhou, L. Luo, Y. Wang, E. Kahng, R. Jin, *J. Am. Chem. Soc.* **2023**, *145*, 19969, <https://doi.org/10.1021/jacs.3c06543>.
- [16] T. D. Green, C. Yi, C. Zeng, R. Jin, S. McGill, K. L. Knappenberger Jr., *J. Phys. Chem. A* **2014**, *118*, 10611, <https://doi.org/10.1021/jp505913j>.
- [17] J. Foxley, T. D. Green, M. A. Tofanelli, C. J. Ackerson, K. L. Knappenberger Jr., *J. Phys. Chem. Lett.* **2023**, *14*, 5210, <https://doi.org/10.1021/acs.jpcllett.3c01170>.
- [18] L. Luo, Z. Liu, X. Du, R. Jin, *J. Am. Chem. Soc.* **2022**, *144*, 19243, <https://doi.org/10.1021/jacs.2c09107>.
- [19] J. Zhao, Université de Genève **2024**, <https://doi.org/10.13097/ARCHIVE-OUVERTE/UNIGE:182170>.
- [20] M. Zhu, W. T. Eckenhoff, T. Pintauer, R. Jin, *CCDC* **2008**, <https://doi.org/10.5517/ccrb6cm>.
- [21] Z. Liu, L. Luo, R. Jin, *Adv. Mater.* **2023**, *2309073*, <https://doi.org/10.1002/adma.202309073>.
- [22] T. D. Green, K. L. Knappenberger, *Nanoscale* **2012**, *4*, 4111, <https://doi.org/10.1039/c2nr31080e>.

- [23] M. A. Tofanelli, K. Salorinne, T. W. Ni, S. Malola, B. Newell, B. Phillips, H. Häkkinen, C. J. Ackerson, *Chem. Sci.* **2016**, *7*, 1882, <https://doi.org/10.1039/C5SC02134K>.
- [24] M. Zhu, W. T. Eckenhoff, T. Pintauer, R. Jin, *J. Phys. Chem. C* **2008**, *112*, 14221, <https://doi.org/10.1021/jp805786p>.
- [25] M. Zhou, C. Yao, M. Y. Sfeir, T. Higaki, Z. Wu, R. Jin, *J. Phys. Chem. C* **2018**, *122*, 13435, <https://doi.org/10.1021/acs.jpcc.7b11057>.
- [26] J. Zhao, A. Ziarati, A. Rosspeintner, Y. Wang, T. Bürgi, *Chem. Sci.* **2023**, *14*, 7665, <https://doi.org/10.1039/D3SC01177A>.
- [27] L. Zhao, J. Luis Pérez Lustres, V. Farztdinov, N. P. Ernsting, *Phys. Chem. Chem. Phys.* **2005**, *7*, 1716, <https://doi.org/10.1039/B500108K>.
- [28] L. Ceresa, J. Kimball, J. Chavez, E. Kitchner, Z. Nurekeyev, H. Doan, J. Borejdo, I. Gryczynski, Z. Gryczynski, *Methods Appl. Fluoresc.* **2021**, *9*, 035005, <https://doi.org/10.1088/2050-6120/ac0243>.
- [29] M. Zhou, Y. Song, *J. Phys. Chem. Lett.* **2021**, *12*, 1514, <https://doi.org/10.1021/acs.jpcclett.1c00120>.

License and Terms



This is an Open Access article under the terms of the Creative Commons Attribution License CC BY 4.0. The material may not be used for commercial purposes.

The license is subject to the CHIMIA terms and conditions: (<https://chimia.ch/chimia/about>).

The definitive version of this article is the electronic one that can be found at <https://doi.org/10.2533/chimia.2026.215>